



Published in final edited form as:

Mov Disord. 2012 June ; 27(7): 864–873. doi:10.1002/mds.25025.

Short latency activation of cortex during clinically effective subthalamic DBS for Parkinson disease

Harrison C. Walker, M.D.^{1,2}, He Huang, M.S.¹, Christopher L. Gonzalez, M.S.¹, Edward Bryant¹, Jeffrey Killen, M.S.¹, Gary C. Cutter, PhD³, Robert C. Knowlton, M.D.¹, Erwin B. Montgomery, M.D.^{1,2}, Bart L. Guthrie, M.D.⁴, and Ray L. Watts, M.D.¹

¹Department of Neurology, University of Alabama at Birmingham; Birmingham, Alabama

²Department of Biomedical Engineering, University of Alabama at Birmingham; Birmingham, Alabama

³Department of Biostatistics, University of Alabama at Birmingham; Birmingham, Alabama

⁴Department of Surgery, Division of Neurosurgery, University of Alabama at Birmingham; Birmingham, Alabama

Abstract

Background—Subthalamic deep brain stimulation is superior to medical therapy for the motor symptoms of advanced Parkinson’s disease, and additional evidence suggests that it improves refractory symptoms of essential tremor, primary generalized dystonia, and obsessive-compulsive disorder. Despite this, its therapeutic mechanism is unknown. We hypothesized that subthalamic stimulation activates cerebral cortex at short latencies after stimulus onset during clinically effective stimulation for Parkinson disease.

Methods—In 5 subjects (6 hemispheres) electroencephalography measured the response of cortex to subthalamic stimulation across a range of stimulation voltages and frequencies. Novel analytical techniques reversed the anode and cathode electrode contacts and summed the resulting pair of event related potentials to suppress the stimulation artifact.

Results—Subthalamic brain stimulation at 20 Hertz activates somatosensory cortex at discrete latencies (mean latencies 1.0 ± 0.4 , 5.7 ± 1.1 , and 22.2 ± 1.8 milliseconds, denoted R1, R2, and R3, respectively). The amplitude of the short latency peak (R1) during clinically effective high frequency stimulation is nonlinearly dependent on stimulation voltage ($p < 0.001$, repeated measures analysis of variance), and its latency is less variable than that of R3 (1.02 versus 19.46 milliseconds, $p < 0.001$, Levene’s test).

Conclusions—Clinically effective subthalamic brain stimulation in humans with Parkinson disease activates cerebral cortex at one millisecond after stimulus onset, most likely by antidromic activation. Our findings suggest that alteration of the precise timing of action potentials in cortical neurons with axonal projections to the subthalamic region is an important component of the therapeutic mechanism of subthalamic brain stimulation.

Introduction

Subthalamic nucleus deep brain stimulation (DBS) is superior to medical therapy for the motor symptoms of Parkinson disease (PD), and additional evidence suggests that it

Corresponding author: Harrison C. Walker, MD, Assistant Professor, Department of Neurology, University of Alabama at Birmingham, 1720 7th Avenue South Birmingham, AL, United States 35294-0017, hcwalker@uab.edu, phone: 205-996-9540, fax: 205-996-4039.

improves refractory symptoms of essential tremor, generalized dystonia, and obsessive-compulsive disorder (1–6). Despite the comparable symptomatic effects of stereotactic lesions (subthalamotomy) and DBS for PD, multiple functional imaging studies show that glucose metabolism / blood flow is increased in the ipsilateral subthalamic nucleus and thalamus and reduced in frontal cortex during effective stimulation versus DBS off (7–10). These paradoxical findings, coupled with electrophysiology showing activation of output structures by DBS, raise the question of whether activation or inhibition of neurons is therapeutically relevant, and whether the mechanism of DBS is a local phenomenon versus a more distributed systems effect (11–15).

Projections from frontal cortex to the subthalamic region (the “hyperdirect” pathway) have been implicated in the pathophysiology of PD and the mechanism of DBS (16–18). In particular, Gradinaru et al. showed improvement in motor function in a mouse model of PD during selective optical activation of frontal cortex neurons and electrical stimulation of the subthalamic region but not during selective optical activation or deactivation of subthalamic neurons alone (19). Although prior electroencephalography (EEG) studies demonstrate event related potentials (ERPs) between 3 to 50 milliseconds after stimulus onset, DBS was delivered at clinically ineffective low frequencies (2–33 Hertz) to avoid the stimulus artifact. This has led some to infer antidromic cortical activation in humans based on the earliest discernable peaks in the ERP and on paired pulse and transcranial magnetic stimulation paradigms, while others argue solely for polysynaptic activation of cortex at longer latencies (20–23). We hypothesized that novel analysis techniques would demonstrate non-synaptic, short latency activation of cortex during clinically effective high frequency subthalamic DBS. Better understanding the mechanism of DBS has the potential to optimize existing therapies and to guide innovation in novel indications in neurology and psychiatry.

Methods

This study received prior Institutional Review Board approval, and subjects were diagnosed with PD based on consensus criteria. Feasibility studies were conducted on 3 subjects, and 5 subjects (6 brain hemispheres) underwent the range of stimulation parameters for the group analyses. Our goal was to characterize the electrophysiology of effective DBS, therefore we enrolled subjects who had the expected postoperative improvement and verified appropriate lead location based on previously published methods (Table 2) (24, 25).

Adjustment to Bipolar Stimulation Configuration and Motor Assessment

A DBS lead consists a linear array of four electrode contacts numbered by convention 0, 1, 2, and 3. Preliminary studies showed that monopolar stimulation elicits a large electrical artifact, therefore subjects were transitioned to bipolar stimulation, using adjacent contacts as anode and cathode. Subjects were blinded to stimulator settings. To verify that similar improvement occurred after the change to bipolar stimulation, we identified the threshold voltage for improvement in the contralateral arm with items 20–25 from the Unified Parkinson Disease Rating Scale (UPDRS). A two-tailed paired t-test evaluated whether motor function changed significantly at this voltage versus DBS off.

Electroencephalographic Recordings

A conventional EEG system measured scalp potentials with subjects awake and at rest. All stimulation epochs and pauses between conditions with DBS off were at least 120 seconds in duration. A second epoch was acquired for each condition following reversal of the anode/cathode pair (i.e., from 2+1- to 2-1+), in random order. The stimulation voltage was increased in 1 Volt increments to 1 Volt above the threshold voltage for motor improvement in the contralateral arm, with the stimulation frequency held constant at 130 Hertz.

Similarly, the stimulation frequency was progressively decreased from higher to lower frequencies, save that the stimulation voltage was held constant at the threshold for motor improvement.

Calculation of Event Related Potentials and Peak Latency and Amplitude Measures

ERPs were calculated by averaging epochs aligned to stimulus onset, and the corresponding anode/cathode pairs were summed to generate a composite ERP for each condition (23). The assumption is that this summation procedure will suppress the stimulus artifact and amplify common elements of the underlying brain response. We generated multiple ERPs within and across conditions by randomly and independently sampling stimulation events without replacement. First, we measured the latencies of the short, intermediate, and long latency peaks in the ERP (denoted R1, R2, and R3 throughout) during 20 Hertz stimulation. Second, we evaluated whether the variance in the peak latency differed between R1 and R3 with Levene's test. Third, EEG field potentials were visualized with both two-dimensional topographic plots and contour plots in individual channels (26). Fourth, we determined whether stimulation voltage and frequency altered the peak amplitude of the short latency response (R1) with repeated measures ANOVA, using the peak amplitude as subject and the stimulation voltage or frequency as condition. If the omnibus statistical tests showed differences at $p < 0.01$, post-hoc comparisons were calculated by the Tukey method. Finally, linear and second-order polynomial regressions on both the millisecond latency peaks and the electrical stimulus transient peaks across stimulation voltages determined which statistical model best explained the data.

Results

Clinical Data and Experimental Stimulator Settings

Demographic data are contained in Table 1. The threshold voltage for motor improvement in the arm was typically approximately 1 Volt higher during bipolar stimulation (regardless of electrode polarity) versus monopolar stimulation, and essentially identical improvement was obtained following anode/cathode reversal.

Polyphasic Event Related Potential to Subthalamic Stimulation

Reversal of the anode and cathode contacts inverts the polarity of the stimulus artifact (green and blue traces, Figure 1), yet both traces demonstrate downgoing (positive) deflections at one millisecond after stimulus onset (R1). Summation of the pair of ERPs minimizes the stimulus artifact and amplifies the underlying brain response (red trace). Similarly, the later peaks in the response at 6 and 22 milliseconds latency (R2 and R3) share the same morphology and timing, regardless of the polarity of the prior stimulation artifact. Across different scalp electrodes, R1 retains the same polarity (red traces), in contrast to phase reversals in the stimulation artifacts (blue and green traces). Furthermore, R1 is not present in EEG electrodes submerged in a bowl of saline with an externalized DBS system (Supplementary Figure 1).

The Short Latency Peak Shows More Precise Timing Than Later Peaks in the ERP

The ERP to subthalamic DBS at 20 Hertz at the threshold voltage for motor improvement in the arm shows three initial peaks across subjects – a temporally fixed early response at 1.0 ± 0.4 milliseconds (R1), a smaller amplitude intermediate latency response at 5.7 ± 1.1 milliseconds (R2), and a broad, longer latency response in 4 of 5 subjects (5 of 6 brain hemispheres) at 22.2 ± 1.8 milliseconds (R3, Figure 2). The variance in peak latency was markedly less for R1 than for R3 (1.0 versus 19.5 milliseconds, $p < 0.001$, Levene's test). Each of the peaks in the ERP showed C3/C4 phase reversals when referenced to the

contralateral mastoid. Furthermore, two-dimensional topographic plots for the stimulus artifact peaks and R1 from the composite ERP indicate that these potentials are spatially independent and cannot localize to the same source, similar to findings from Figure 1.

The Amplitude of the Short Latency Peak Depends Non-linearly on Stimulation Voltage

The amplitude of R1 increases with stimulation voltage, with stimulation frequency held constant at 130 Hz. Contour plots from EEG electrodes in one subject demonstrate the instantaneous, reproducible nature of the response and its stable latency across DBS voltages (Figure 3). Regression demonstrates that the peak amplitude of R1 as a function of stimulation voltage was best fit by a second order polynomial, while the stimulus artifact peak was best fit by simple linear regression. Furthermore, repeated measures ANOVA shows a significant effect of stimulation voltage on the amplitude of the response ($p < 0.001$), and post-hoc paired comparisons showed differences in amplitudes across stimulation voltages. Importantly, improvement in motor symptoms in the contralateral arm was demonstrated across subjects at the threshold voltage during high frequency stimulation ($p = 0.002$).

Similar contour plots illustrate the relationship between stimulation frequency and the ERP over short time scales, with the stimulation voltage held constant at the threshold for motor improvement (Figure 4). The later peaks in the response are not visible at higher stimulation frequencies, because they are obscured by the subsequent stimulus pulses. In contrast to its relationship to stimulation voltage, R1 is present across the range of stimulation frequencies. Repeated measures ANOVA showed evidence for smaller R1 peak amplitudes at the highest stimulation frequencies ($p = 0.012$), and post-hoc analyses showed highly significant within-subject effects of stimulation frequency on R1 amplitude ($p < 0.001$).

In summary, the following observations indicate that R1 is not an electrical artifact: (1) within individual EEG electrodes, its polarity is independent from the preceding stimulus artifact when the anode and cathode DBS contacts are reversed; (2) across different EEG electrodes, its spatial localization is independent from the stimulus artifact; (3) it is not observed in a bowl of saline containing an externalized DBS system; (4) its peak has the same polarity as the later peaks in the response during low frequency DBS; and finally (5) its amplitude increases non-linearly with rising stimulation voltages in contrast to the stimulus artifact.

Discussion

Our results demonstrate that neurons in cerebral cortex discharge at one millisecond after the stimulus pulse during clinically effective high frequency subthalamic DBS in humans with PD. This most likely represents a non-synaptic, antidromic (retrograde) response, based on the following observations: (1) it occurs too rapidly for synaptic transmission; (2) its latency is more fixed than later peaks in the response; and (3) it is present across a range of stimulation frequencies. Furthermore, our findings suggest this potential localizes to ipsilateral cortex, which parallels results of Gradinaru et. al., who demonstrated that optical activation of cortical neurons and subthalamic stimulation, but not activation or deactivation of subthalamic neurons alone, improved motor function in a mouse model of PD (19).

The short latency response (R1) is conducted over an approximate distance of 6 centimeters between the subthalamic region and the cortical surface, suggesting a conduction velocity of at least 60 meters/second. Although this rapid velocity is consistent with retrograde activation of large diameter cortical pyramidal cell axons, a caveat is that we cannot demonstrate collision because these were non-invasive scalp potentials from humans with idiopathic PD. Despite this, prior animal studies have demonstrated antidromic cortical

discharges and collision during subthalamic electrical stimulation (17). Another potential contributor to R1 might be the summed orthodromic depolarization of presynaptic axon terminals in cortex originating from the subthalamic region, prior to the generation of the excitatory post-synaptic potential (26). This is less likely, however, because the peak at one millisecond occurs considerably sooner than the predicted latency for the slower conducting, smaller diameter axons of subthalamic neurons (~5–8 milliseconds) (18, 27, 28). Furthermore, it is unclear to what extent EEG can detect presynaptic axonal depolarizations (29).

Our methods to minimize the stimulation artifact demonstrate the morphology and timing of R1 from its onset, suggesting that the later peaks measured by Kuriakose et. al. and others at 3 milliseconds latency represents the conclusion or “tail” of the waveform (20). Indeed, our results demonstrate that stimulus artifact obscures most, if not all, of R1 in prior EEG studies. Our latencies are also faster than those measured during antidromic activation of cortical neurons in rodents (~1.6 ms) (17). This is likely based upon the following: (1) isoflurane and ketamine were used together for anesthesia, both of which slow the conduction velocity (30, 31); (2) the brain may have been cooled towards the ambient temperature during surgical exposure, further slowing the conduction velocity (28); and (3) stimulation artifact may have obscured the fastest responses. Regardless of these mechanistic and technical considerations, our results demonstrate a short latency scalp potential that is associated with symptomatically effective, high frequency subthalamic DBS in humans with idiopathic PD.

Contrary to predictions of stereotactic lesions (subthalamotomy), multiple functional imaging studies demonstrate both increased activity in the ipsilateral subthalamic nucleus and thalamus and reduced activity in frontal cortex during effective subthalamic DBS versus no stimulation (32). Furthermore, Haslinger et. al. show that increasing stimulation frequencies result in corresponding decreases in glucose metabolism in ipsilateral frontal cortex (33). Assuming that subthalamic stimulation activates “hyperdirect” pathway axons bidirectionally, our results suggest that in addition to antidromic cortical activation, DBS alters the precise timing and magnitude of orthodromic discharges to the subthalamic region as well (34). This inference addresses the paradoxical functional imaging findings, particularly given that animal studies have shown that non-synaptic, antidromic activation of cell bodies (in this case in frontal cortex) is likely metabolically less demanding than synaptic, orthodromic activation of pre- and post-synaptic terminals (in the subthalamic region) (35–37). So regardless of whether the cortical potential itself has mechanistic importance, it may serve as a biomarker for stimulation-related orthodromic activation of the subthalamic region. Interestingly, clinical studies suggest that the most effective DBS contacts are located just dorsal to the subthalamic nucleus rather than within or below it, consistent with the notion that motor improvement is associated with depolarization of axons descending from cortex into the subthalamic region (38, 39).

The more variable timing of the later peaks (R2 and R3) versus R1 suggests that they represent orthodromic, synaptic activity. Our methods have allowed discrimination of a distinct peak at an intermediate latency of 5.7 milliseconds (R2), the timing of which is compatible with monosynaptic, orthodromic activity measured in primate subthalamic neurons upon stimulation in the opposite direction from ipsilateral frontal cortex to subthalamic neurons (5.8 milliseconds) (40, 41). The broad, temporally dispersed response at approximately 22 milliseconds latency (R3) most likely represents polysynaptic activation of cortex, which may originate from activation of pallidothalamic fibers in or around the zona incerta. Other possible contributors to both of these later responses include phase resetting by antidromic activation followed by synchronized spontaneous discharges, local processing via cortico-cortical synapses or interneurons, or activation of other anatomical

pathways. Regardless, neuronal synchronization, resonance, beat phenomena, and oscillations have been proposed as potential components of the therapeutic mechanism of DBS (13, 15, 42, 43).

The peak amplitude of R1 is non-linearly dependent on the DBS voltage during high frequency stimulation. This suggests that increasing stimulation voltages activate correspondingly larger tissue volumes, the number of available axons within which would be expected to increase exponentially. The geometry of this volume is likely complex and dependent upon on local impedances, electrode location, stimulation parameters, and other variables (44). Additionally, the range and/or step size between voltages may limit more detailed inferences regarding this relationship. In contrast to voltage, stimulation frequency had a less prominent effect on the peak amplitude of the antidromic potential, trending towards smaller amplitudes at higher frequencies at the group level ($p = 0.012$). This preliminary finding suggests that cortical neurons with efferent axons in the subthalamic region are more likely to be refractory at the time of a given stimulus pulse during effective high frequency DBS versus lower frequency stimulation (12).

This study has potential limitations, many of which were imposed by efforts to balance the duration and tolerability of the protocol in these advanced PD patients without DBS and dopaminergic medications for greater than 12 hours. First, although motor function was not quantified at the lower stimulation frequencies and voltages, we demonstrated significant improvement in the UPDRS score for the contralateral arm at the threshold stimulation voltage versus DBS off, which verifies that the bipolar stimuli were of sufficient intensity to provide symptomatic improvement. Second, the short stimulation epochs might temporarily improve motor function or cause carry-over effects, however tremor and rigidity typically change within seconds of DBS activation/inactivation, and 60–80% of bradykinesia returns within 60 seconds of inactivation (45, 46). Although these durations are well within our time intervals, motor improvement still might not be sustained hours or days after the acute stimulator adjustments. Third, anatomically ineffective locations were not stimulated, however DBS was delivered at ineffective/suboptimal settings from appropriately located contacts (i.e., all of the lower stimulation voltages and frequencies). Fourth, since the amplitudes of the composite ERPs represent the sum of pairs of responses, the reported values are larger than what would be expected from a single stimulation condition. Fifth, although the number of subjects enrolled was relatively small, our findings were consistent across subjects, and high stimulation frequencies allowed the generation of independent ERPs for within-subject comparisons, thereby improving statistical power. Finally, the extent to which cortico-subthalamic axons arise as collateral projections from the corticospinal tract versus originating from distinct populations of cortical neurons is unclear. Although some portion of the R1 might arise from direct activation of descending corticospinal tract axons or other fibers of passage, multiple observations argue against direct corticospinal tract activation, including electromyography data which do not show temporally fixed, short latency responses in the contralateral arm during DBS (see Supplementary Figure 2).

In summary, we found that effective high frequency subthalamic DBS for PD is associated with synchronization of cortical neurons at the stimulation frequency or one of its sub-harmonics. Furthermore, assuming that cortico-subthalamic axons are activated bidirectionally, stimulation likely alters the precise timing and magnitude of “hyperdirect” pathway discharges in the subthalamic region, as well. Since DBS systems offer more settings that can be practically tested in the research or clinical environment, one therapeutic implication is that similar techniques could allow estimation of the physiological dose of DBS the brain, which could confer greater or more sustained efficacy, fewer adverse effects, fewer follow-up appointments for stimulator readjustment, less frequent surgery for battery

depletion, and lower cost. Furthermore, while a visible symptom like tremor typically responds to effective stimulation within seconds, patients with dystonia, psychiatric diseases, and novel proposed indications for DBS may not experience maximal clinical effects until days or weeks after stimulation is begun.

Supplementary Material

Refer to Web version on PubMed Central for supplementary material.

Acknowledgments

The authors acknowledge the patients who volunteered to participate in this research. This work was supported by the United States National Institutes of Health [K23-NS067053-01 to H.C.W.]; and the American Parkinson Disease Association [H.C.W.]. E.B.M. has received consulting fees from St. Jude Neuromodulation.

References

1. Weaver FM, Follett K, Stern M, Hur K, Harris C, Marks WJ Jr, et al. Bilateral deep brain stimulation vs best medical therapy for patients with advanced parkinson disease: A randomized controlled trial. *JAMA*. 2009 Jan 7; 301(1):63–73. [PubMed: 19126811]
2. Mallet L, Polosan M, Jaafari N, Baup N, Welter ML, Fontaine D, et al. Subthalamic nucleus stimulation in severe obsessive-compulsive disorder. *N Engl J Med*. 2008 Nov 13; 359(20):2121–34. [PubMed: 19005196]
3. Lind G, Schechtmann G, Lind C, Winter J, Meyerson BA, Linderoth B. Subthalamic stimulation for essential tremor. short- and long-term results and critical target area. *Stereotact Funct Neurosurg*. 2008; 86(4):253–8. [PubMed: 18552522]
4. Kleiner-Fisman G, Liang GS, Moberg PJ, Ruocco AC, Hurtig HI, Baltuch GH, et al. Subthalamic nucleus deep brain stimulation for severe idiopathic dystonia: Impact on severity, neuropsychological status, and quality of life. *J Neurosurg*. 2007 Jul; 107(1):29–36. [PubMed: 17639870]
5. Deuschl G, Schade-Brittinger C, Krack P, Volkmann J, Schafer H, Botzel K, et al. A randomized trial of deep-brain stimulation for parkinson's disease. *N Engl J Med*. 2006 Aug 31; 355(9):896–908. [PubMed: 16943402]
6. Plaha P, Patel NK, Gill SS. Stimulation of the subthalamic region for essential tremor. *J Neurosurg*. 2004 Jul; 101(1):48–54. [PubMed: 15255251]
7. Geday J, Ostergaard K, Johnsen E, Gjedde A. STN-stimulation in parkinson's disease restores striatal inhibition of thalamocortical projection. *Hum Brain Mapp*. 2009 Jan; 30(1):112–21. [PubMed: 18041743]
8. Karimi M, Golchin N, Tabbal SD, Hershey T, Videen TO, Wu J, et al. Subthalamic nucleus stimulation-induced regional blood flow responses correlate with improvement of motor signs in parkinson disease. *Brain*. 2008 Aug 12.
9. Trost M, Su S, Su P, Yen RF, Tseng HM, Barnes A, et al. Network modulation by the subthalamic nucleus in the treatment of parkinson's disease. *Neuroimage*. 2006 May 15; 31(1):301–7. [PubMed: 16466936]
10. Asanuma K, Tang C, Ma Y, Dhawan V, Mattis P, Edwards C, et al. Network modulation in the treatment of parkinson's disease. *Brain*. 2006 Oct; 129(Pt 10):2667–78. [PubMed: 16844713]
11. Hashimoto T, Elder CM, Okun MS, Patrick SK, Vitek JL. Stimulation of the subthalamic nucleus changes the firing pattern of pallidal neurons. *J Neurosci*. 2003 Mar 1; 23(5):1916–23. [PubMed: 12629196]
12. Chomiak T, Hu B. Axonal and somatic filtering of antidromically evoked cortical excitation by simulated deep brain stimulation in rat brain. *J Physiol*. 2007 Mar 1; 579(Pt 2):403–12. [PubMed: 17170044]
13. Hammond C, Ammari R, Bioulac B, Garcia L. Latest view on the mechanism of action of deep brain stimulation. *Mov Disord*. 2008 Sep 10.

14. Carlson JD, Cleary DR, Cetas JS, Heinricher MM, Burchiel KJD. Deep brain stimulation (DBS) does not silence neurons in subthalamic nucleus in parkinson's patients. *J Neurophysiol.* 2009 Dec 2.
15. Walker HC, Watts RL, Schrandt CJ, Huang H, Guthrie SL, Guthrie BL, et al. Activation of subthalamic neurons by contralateral subthalamic deep brain stimulation in parkinson disease. *J Neurophysiol.* 2010 Dec 22.
16. Nambu A, Tokuno H, Takada M. Functional significance of the cortico-subthalamo-pallidal 'hyperdirect' pathway. *Neurosci Res.* 2002 Jun; 43(2):111–7. [PubMed: 12067746]
17. Li S, Arbuthnott GW, Jutras MJ, Goldberg JA, Jaeger D. Resonant antidromic cortical circuit activation as a consequence of high-frequency subthalamic deep-brain stimulation. *J Neurophysiol.* 2007 Dec; 98(6):3525–37. [PubMed: 17928554]
18. Braak H, Del Tredici K. Cortico-basal ganglia-cortical circuitry in parkinson's disease reconsidered. *Exp Neurol.* 2008 Jul; 212(1):226–9. [PubMed: 18501351]
19. Gradinaru V, Mogri M, Thompson KR, Henderson JM, Deisseroth K. Optical deconstruction of parkinsonian neural circuitry. *Science.* 2009 Apr 17; 324(5925):354–9. [PubMed: 19299587]
20. Ashby P, Paradiso G, Saint-Cyr JA, Chen R, Lang AE, et al. Potentials recorded at the scalp by stimulation of the subthalamic nucleus. *Clin Neurophysiol.* 2001 Mar; 112(3):431–1. [PubMed: 11222963]
21. Kuriakose R, Saha U, Castillo G, Udupa K, Ni Z, Gunraj C, et al. The nature and time course of cortical activation following subthalamic stimulation in parkinson's disease. *Cereb Cortex.* 2009 Dec 17.
22. MacKinnon CD, Webb RM, Silberstein P, Tisch S, Asselman P, Limousin P, et al. Stimulation through electrodes implanted near the subthalamic nucleus activates projections to motor areas of cerebral cortex in patients with parkinson's disease. *Eur J Neurosci.* 2005 Mar; 21(5):1394–402. [PubMed: 15813949]
23. Baker KB, Montgomery EB Jr, Rezai AR, Burgess R, Luders HO. Subthalamic nucleus deep brain stimulus evoked potentials: Physiological and therapeutic implications. *Mov Disord.* 2002 Sep; 17(5):969–83. [PubMed: 12360546]
24. Walker HC, Watts RL, Guthrie S, Wang D, Guthrie BL. Bilateral effects of unilateral subthalamic deep brain stimulation on parkinson's disease at 1 year. *Neurosurgery.* 2009 Aug; 65(2):302,9. discussion 309–10. [PubMed: 19625909]
25. Shenai MB, Walker H, Guthrie S, Watts R, Guthrie BL. Construction of relational topographies from the quantitative measurements of functional deep brain stimulation using a 'roving window' interpolation algorithm. *Stereotact Funct Neurosurg.* 2010; 88(1):16–23. [PubMed: 19940545]
26. Delorme A, Makeig S. EEGLAB: An open source toolbox for analysis of single-trial EEG dynamics including independent component analysis. *J Neurosci Methods.* 2004 Mar 15; 134(1): 9–21. [PubMed: 15102499]
27. Degos B, Deniau JM, Le Cam J, Mailly P, Maurice N. Evidence for a direct subthalamo-cortical loop circuit in the rat. *Eur J Neurosci.* 2008 May; 27(10):2599–610. [PubMed: 18547246]
28. Debanne D, Campanac E, Bialowas A, Carlier E, Alcaraz G. Axon physiology. *Physiol Rev.* 2011; 91(2):555–602. [PubMed: 21527732]
29. Olejniczak P. Neurophysiologic basis of EEG. *J Clin Neurophysiol.* 2006; 23:186–9. [PubMed: 16751718]
30. Ozaki S, Nakaya H, Gotoh Y, Azuma M, Kemmotsu O, et al. Effects of isoflurane on conduction velocity and maximum rate of rise in guinea pig papillary muscles. *Anesth Analg.* 1990; 70(6): 618–23. [PubMed: 2344056]
31. Hara Y, Tamagawa M, Nakaya H. The effects of ketamine on conduction velocity and maximum rate of rise of upstroke in guinea pig papillary muscles: comparison with quinidine. *Anesth Analg.* 1994; 79(4):687093.
32. Boertien T, Zrinzo L, Kahan J, Jahanshahi M, Hariz M, Mancini L, et al. Functional imaging of subthalamic nucleus deep brain stimulation in Parkinson's disease. *Mov Disord.* 2011 Jun 14. [Epub ahead of print].

33. Haslinger B, Kalteis K, Boecker H, Alesch F, Ceballos-Baumann AO. Frequency-correlated decreases of motor cortex activity associated with subthalamic nucleus stimulation in parkinson's disease. *Neuroimage*. 2005 Nov 15; 28(3):598–606. [PubMed: 16081302]
34. Eccles JC, Granit R, Young JZ. Impulses in the giant fibers of earthworms. *J Physiol*. 1933; 77:23–4.
35. Kadekaro M, Vance WH, Terrell ML, Gary H Jr, Eisenberg HM, Sokoloff L. Effects of antidromic stimulation of the ventral root on glucose utilization in the ventral horn of the spinal cord in the rat. *Proc Natl Acad Sci U S A*. 1987 Aug; 84(15):5492–5. [PubMed: 3474665]
36. Jueptner M, Weiller C. Review: Does measurement of regional cerebral blood flow reflect synaptic activity? implications for PET and fMRI. *Neuroimage*. 1995 Jun; 2(2):148–56. [PubMed: 9343597]
37. Logothetis NK. What we can do and what we cannot do with fMRI. *Nature*. 2008 Jun 12; 453(7197):869–78. [PubMed: 18548064]
38. Zheng Z, Zhang YQ, Li JY, Zhang XH, Zhuang P, Li YJ. Subthalamic deep brain stimulation for parkinson's disease: Correlation of active contacts and electrophysiologically mapped subthalamic nucleus. *Chin Med J (Engl)*. 2009 Oct 20; 122(20):2419–22. [PubMed: 20079152]
39. Johnsen EL, Sunde N, Mogensen PH, Ostergaard K. MRI verified STN stimulation site--gait improvement and clinical outcome. *Eur J Neurol*. 2010 May; 17(5):746–53. [PubMed: 20345927]
40. Nambu A, Tokuno H, Hamada I, Kita H, Imanishi M, Akazawa T, et al. Excitatory cortical inputs to pallidal neurons via the subthalamic nucleus in the monkey. *J Neurophysiol*. 2000 Jul; 84(1): 289–300. [PubMed: 10899204]
41. Jackson A, Crossman AR. Subthalamic nucleus efferent projection to the cerebral cortex. *Neuroscience*. 1981; 6(11):2367–77. [PubMed: 7329552]
42. Cooper SE, Kuncel AM, Wolgamuth BR, Rezai AR, Grill WM. A model predicting optimal parameters for deep brain stimulation in essential tremor. *J Clin Neurophysiol*. 2008 Oct; 25(5): 265–73. [PubMed: 18791473]
43. Montgomery EB Jr, Gale JT. Mechanisms of action of deep brain stimulation(DBS). *Neurosci Biobehav Rev*. 2008; 32(3):388–407. [PubMed: 17706780]
44. McIntyre CC, Grill WM, Sherman DL, Thakor NV. Cellular effects of deep brain stimulation: Model-based analysis of activation and inhibition. *J Neurophysiol*. 2004 Apr; 91(4):1457–69. [PubMed: 14668299]
45. Moro E, Esselink RJ, Xie J, Hommel M, Benabid AL, Pollak P. The impact on parkinson's disease of electrical parameter settings in STN stimulation. *Neurology*. 2002 Sep 10; 59(5):706–13. [PubMed: 12221161]
46. Kereszteni Z, Valkovic P, Eggert T, Steude U, Hermsdorfer J, Laczko J, et al. The time course of the return of upper limb bradykinesia after cessation of subthalamic stimulation in parkinson's disease. *Parkinsonism Relat Disord*. 2007 Oct; 13(7):438–42. [PubMed: 17292654]

Appendix

Author Roles

1. Research project: A. Conception, B. Organization, C. Execution.
2. Statistical Analysis: A. Design, B. Execution, C. Review and Critique.
3. Manuscript: A. Writing of the first draft, B. Review and Critique.

Harrison Walker - 1A, 1B, 1C, 2A, 2B, 2C, 3A, 3B

He Huang - 1C, 2A, 2B, 2C, 3B

Christopher Gonzalez - 1B, 1C, 2B, 2C, 3B

James Bryant - 1A, 2A, 2B, 2C, 3B

Jeff Killen - 1A, 1C, 3B

Gary Cutter - 2A, 2B, 2C, 3B

Robert Knowlton - 1A, 1C, 2C, 3B

Erwin Montgomery - 1A, 1C, 2A, 2C, 3B

Bart Guthrie - 1A, 2A, 2C, 3B

Ray Watts - 1A, 2A, 2C, 3B

Financial Disclosures Over the Past Year

Harrison Walker

Stock Ownership (medically related):	none
Intellectual Property Rights:	none
Consultancies:	none
Expert Testimony:	none
Advisory Boards:	none
Employment:	University of Alabama at Birmingham
Partnerships:	none
Contracts:	none
Honoraria:	University of South Florida CME
Royalties:	none
Grants:	National Institutes of Health, K23 NS067053-01, PI
Other:	none

He Huang

Stock Ownership (medically related):	none
Intellectual Property Rights:	none
Consultancies:	none
Expert Testimony:	none
Advisory Boards:	none
Employment:	University of Alabama at Birmingham
Partnerships:	none
Contracts:	none
Honoraria:	none
Royalties:	none
Grants:	none
Other:	none

Chris Gonzalez

Stock Ownership (medically related):	none
Intellectual Property Rights:	none
Consultancies:	none
Expert Testimony:	none
Advisory Boards:	none

Employment:	University of Alabama at Birmingham
Partnerships:	none
Contracts:	none
Honoraria:	none
Royalties:	none
Grants:	none
Other:	none

James Bryant

Stock Ownership (medically related):	none
Intellectual Property Rights:	none
Consultancies:	none
Expert Testimony:	none
Advisory Boards:	none

Employment:	University of Alabama at Birmingham
Partnerships:	none
Contracts:	none
Honoraria:	none
Royalties:	none
Grants:	none
Other:	none

Jeff Killen

Stock Ownership (medically related):	none
Intellectual Property Rights:	none
Consultancies:	none
Expert Testimony:	none
Advisory Boards:	none

Employment:	University of Alabama at Birmingham
Partnerships:	none
Contracts:	none
Honoraria:	none
Royalties:	none
Grants:	none
Other:	none

Gary Cutter

Stock Ownership (medically related):	none
Intellectual Property Rights:	none

Consultancies / Advisory boards:	Alexion Bayhill Bayer Celgene Novartis Genzyme Klein-Buendel Incorporated Nuron Biotech Peptimmune Somnus Pharmaceuticals Sandoz Teva pharmaceuticals UTSouthwestern Visioneering Technologies, Inc
----------------------------------	---

Expert Testimony:	none
-------------------	------

Employment:	University of Alabama at Birmingham
Partnerships:	none
Contracts:	none
Honoraria:	none

Royalties: none
 Grants: Consortium of MS Centers
 Data/safety monitoring committees: Sanofi-Aventis Cleveland Clinic Daichi-Sankyo Glaxo Smith Klein Genmab
 Biopharmaceuticals Eli Lilly Medivation Modigenetech Ono
 Pharmaceuticals PTC Therapeutics Teva Vivus Univ of Penn NHLBI
 NINDS NMSS

Other: none

Robert Knowlton

Stock Ownership (medically related): none
 Intellectual Property Rights: none
 Consultancies: Lundbeck
 Expert Testimony: none
 Advisory Boards: none
 Employment: University of Alabama at Birmingham
 Partnerships: none
 Contracts: none
 Honoraria: UCB Pharma
 Royalties: none
 Grants: none
 Clinical trials: Eisai
 Other: none

Erwin Montgomery

Stock Ownership (medically related): none
 Intellectual Property Rights: none
 Consultancies: St. Jude Neuromodulation Boston Scientific
 Expert Testimony: none
 Advisory Boards: American Parkinson Disease Association ST/Dystonia Inc.
 Employment: University of Alabama at Birmingham Birmingham Veterans Affairs
 Medical Center
 Partnerships: none
 Contracts: none
 Honoraria: Movement Disorders Society International Congress European Society for
 Stereotatic and Functional Neurosurgery University of South Florida CME
 Korean Movement Disorders Society
 Royalties: Deep Brain Stimulation: Principles and Practice (book)
 Grants: none
 Clinical trials: none
 Other: none

Bart Guthrie

Stock Ownership (medically related): Vipaar
 Intellectual Property Rights: none
 Consultancies: none
 Expert Testimony: yes
 Advisory Boards: none
 Employment: University of Alabama at Birmingham Birmingham Veterans Affairs
 Medical Center

Partnerships:	none
Contracts:	none
Honoraria:	none
Royalties:	none
Grants:	NIBIB
Other:	none

Ray Watts

Stock Ownership (medically related):	none
Intellectual Property Rights:	none
Consultancies:	none
Expert Testimony:	none
Advisory Boards:	Teva Pharmaceuticals UCB Pharma Ipsen
Employment:	University of Alabama at Birmingham
Partnerships:	none
Contracts:	none
Honoraria:	none
Royalties:	Movement Disorders (textbook)
Grants:	Ceregene, Inc.
Other:	none

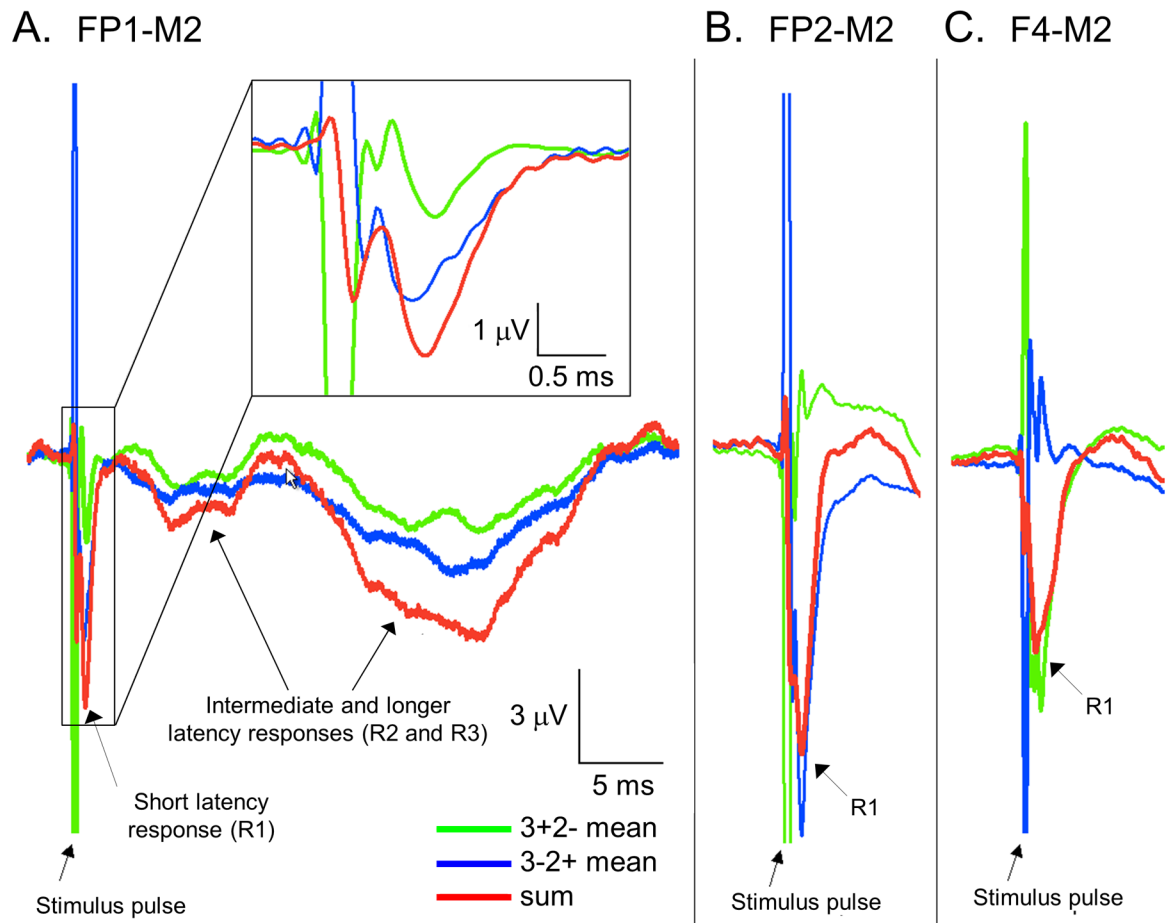


Figure 1. The short latency response to subthalamic DBS and the electrical stimulus transient are independent signals

(A) Within a single EEG electrode, responses from FP1-M2 during 20 Hertz left subthalamic DBS show reversal of the stimulus artifact by inversion of the anode and cathode contacts (3+2- and 3-2+, blue and green traces, respectively). The composite ERP demonstrate three discrete peaks at approximate latencies of 1, 6 and 22 milliseconds after stimulus onset (P1, P2, and P3, respectively, red traces). The inset shows the short latency response over a shorter time scale, demonstrating that it retains the same polarity, regardless of the polarity of the bipolar stimulus transient that precedes it. Furthermore, the polarity of the millisecond latency peak shares the same polarity as the later peaks in the response, both in the two anode/cathode pairings (blue and green traces) and in the composite ERP (red trace). (B, C) Across different EEG electrodes, the electrical stimulus transients (blue and green traces) but not the short latency brain response (red traces) in F4-M2 are reversed relative to FP1-M2 and FP2-M2, indicating that the stimulus artifact from the DBS pulse (the large peaks in the blue and green traces) and the short latency brain response (red traces) are spatially independent and cannot localize to the same source. Each trace is the average of approximately 9000 stimulation events in each of the anode-cathode pairings.

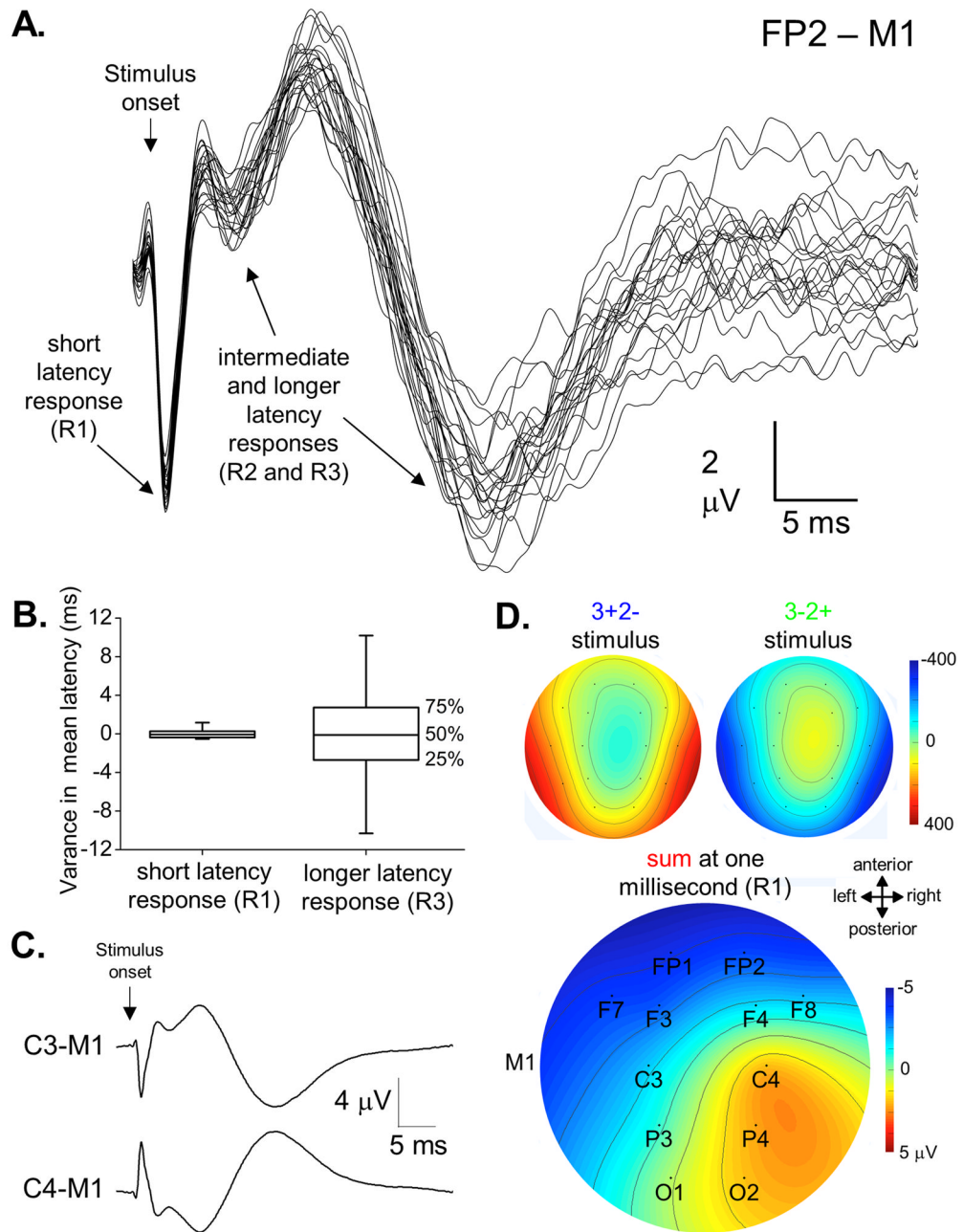


Figure 2. Event related potential to subthalamic DBS

(A) Multiple responses from subthalamic DBS in one subject are calculated from independent stimuli within each condition (right subthalamic DBS at 20 Hertz, each trace is the average of approximately 100 stimulation events in the two anode-cathode pairings). (B) Box plots demonstrate that the variance in peak latency is considerably less for the short latency response (P1) versus the later peak at approximately 22 milliseconds after stimulus onset across all subjects (P3, $p < 0.001$, Levene's test). (C) Although localization was not the primary aim of this study, C3/C4 phase reversals were typically seen in each of the peaks in the ERP (each trace is the average of more than 2,000 stimulation events for each anode/cathode pairing). (D) Topographic plots of EEG field potentials both for the stimulus artifact and the short latency brain response. The pair of stimulus artifacts show the expected

polarity inversion and presumably localize subcortically where current exits the DBS electrode. In contrast, the short latency brain response shows a C3/C4 phase reversal ipsilateral to the DBS, suggesting localization to somatosensory cortex.

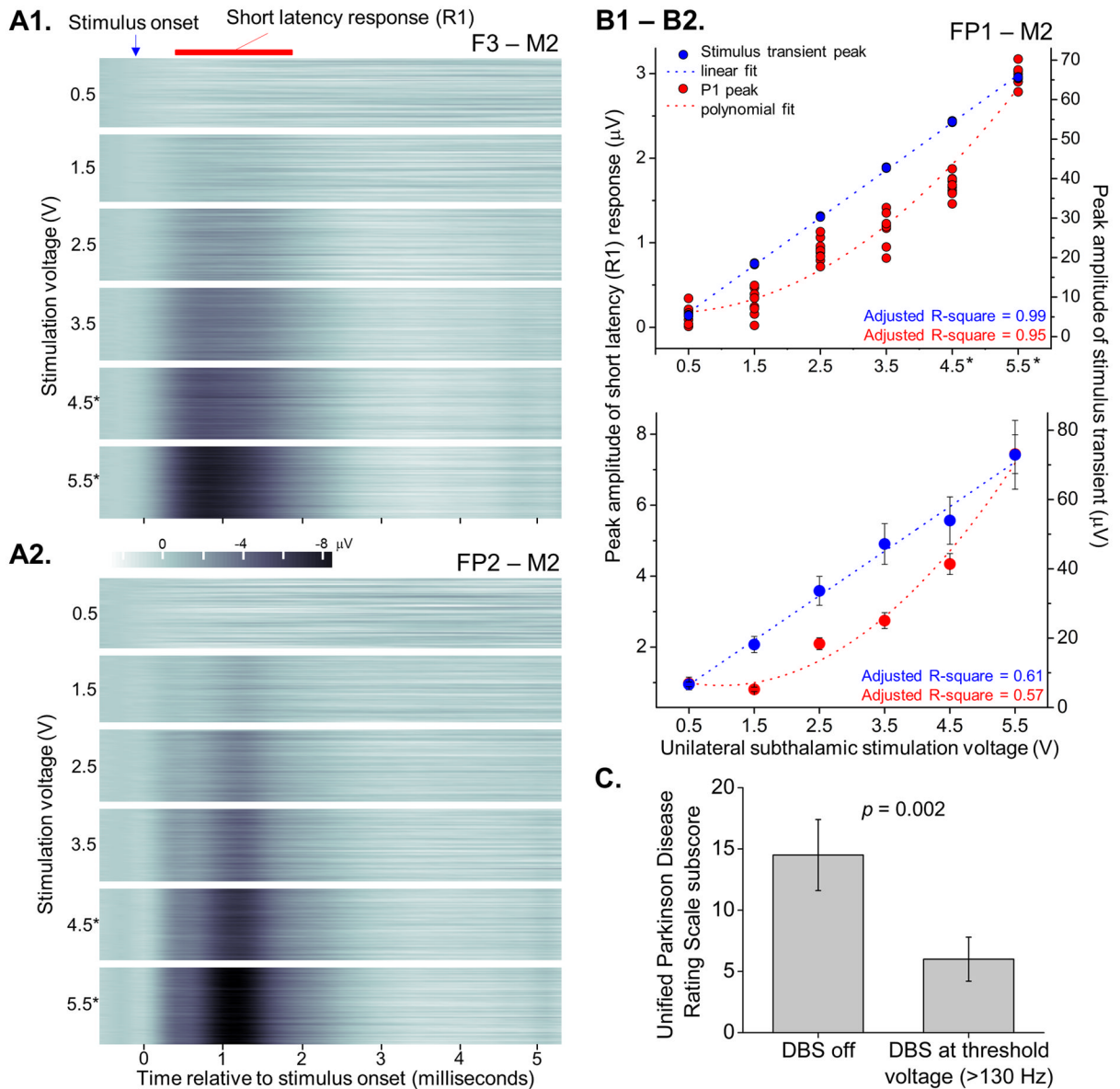


Figure 3. The peak amplitude of the short latency response (R1) increases nonlinearly with stimulation voltage and is present during clinically effective high frequency stimulation Throughout this figure, asterisks indicate the stimulation voltages associated with improvement in motor symptoms in the contralateral arm. **(A1)** Contour plots demonstrate composite ERPs in F3-M2 with peak latencies of approximately 0.8 milliseconds after stimulus onset delivered across a range of stimulation voltages, at constant frequency and pulse width of 185 Hz and 60 μV , respectively. **(A2)** In the same subject, the peak of the short latency response occurs slightly later, at approximately 1.1 ms, in channel FP2-M2 (the plots consist of 50 ERPs per stimulation voltage, each an average of approximately 50 stimulation events). **(B1)** Peak amplitudes of the short latency response (red dots) and the stimulus artifact (blue dots) in an additional subject across the range of stimulation voltages, with corresponding linear and polynomial regressions (dotted lines, 10 ERPs per stimulation voltage, each generated from approximately 150 stimulation events). Individual blue dots are sometimes not discernable because they overlap one another so closely. **(B2)** Linear and

polynomial regressions across all subjects. (C) Significant improvement in tremor, rigidity, and bradykinesia in the contralateral arm occurred at the threshold stimulation voltage during high frequency stimulation versus DBS off ($p = 0.002$, paired t-test).

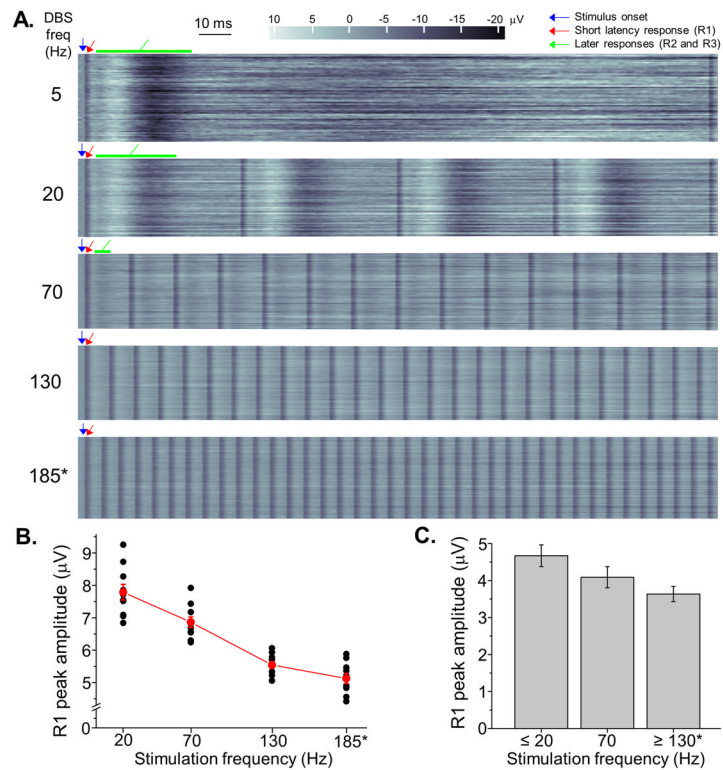


Figure 4. Event related potentials to subthalamic DBS are altered by stimulation frequency
 Throughout this figure, asterisks indicate the stimulation conditions associated with improvement in motor symptoms in the contralateral arm. **(A)** ERPs to subthalamic DBS depicted in contour plots in a subject across a range of stimulation frequencies, with voltage and pulse width held constant at 4.5 Volts and 60 milliseconds, respectively. Blue arrows denote the onset time of the electrical stimulus transient, which is eliminated by the analysis procedure. The short latency cortical response (R1) is present across all stimulation frequencies (the narrow vertical bars in the contour plots, initial responses denoted by red arrows), and the longer latency components of the ERP (R2 and R3, green arrows) are prominent during the lower frequency stimulation conditions (5, 20, and 70 Hz). These later responses diminish in amplitude during 20 Hz versus 5 Hz stimulation and are obscured by ensuing stimulus pulses at progressively higher stimulation frequencies (approximately 50 ERPs per condition). **(B)** The peak amplitude of the short latency response diminishes at higher stimulation frequencies in an individual subject (10 ERPs at each DBS frequency, repeated measures ANOVA, $p < 0.001$), and **(C)** across all subjects there was also evidence for diminished amplitude of the short latency ERP at higher stimulation frequencies (repeated measures ANOVA, $p = 0.012$).

TABLE 1

Subject number	Home stimulator settings		Experimental stimulator settings										
	Age* (years)	Disease duration (years)	Side	Anode / Cathode	Voltage (V)	Pulse width (μ s)	Frequency (Hz)	Anode / Cathode pair		Voltage threshold (volts)		Pulse width (μ s)	Frequency (Hz)
								dorsal	ventral	dorsal	ventral		
1	60	16	Left	Case	2	3.3	60	3	2	4.5	4.5	60	185
2	70	16	Right	Case	2	3.5	60	3	2	4.5	4.5	60	160
3	50	8	Right	Case	3	3.0	60	3	2	3.5	3.5	60	130
4	60	12	Left	Case	1	4.4	120	2	1	4.5	4.5	120	160
5	50	8	Left	Case	2	2.8	60	3	2	3.5	3.5	60	160
6	50	8	Right	Case	2	3.3	90	3	2	4.5	3.5	90	130
Mean (SD)	63.0 (9.2)	11.0 (3.9)											

* rounded to nearest decade

TABLE 2

Subject number	Electrode contact pair used in protocol	Coordinates of electrode contacts relative to anterior commissure - posterior commissure midpoint (millimeters)			EEG electrode
		X	Y	Z	
1	3	11.5	0.1	-0.5	FP1 - M1
	2	11.1	-1.5	2.0	
2	3	14.7	0.3	4.1	F8 - M1
	2	14.3	-1.3	1.6	
3	3	-14.8	-0.2	-4.3	FP1 - M2
	2	-14.2	-1.4	-1.6	
4	2	-12.7	-3.0	-2.5	F8 - M2
	1	-12.1	-4.4	-5.1	
5	3	-13.5	0.2	0.5	F4 - M2
	2	-13.0	-1.4	-2.0	
6	3	12.3	-3.5	-4.3	F3 - M1
	2	13.4	-1.9	-2.0	
	Mean (SEM)	13.1* (0.4)	-1.5 (0.4)	-1.5 (0.8)	

* mean of the absolute value of X to account for brain hemisphere